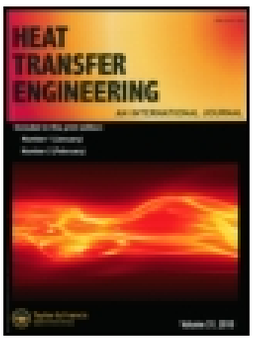

Heat Transfer Engineering

ISSN: 0145-7632 (Print) 1521-0537 (Online) Journal homepage: http://www.tandfonline.com/loi/uhte20

Point Thermal Transmittance of Rib Intersections in Concrete Sandwich Wall Panels

Marta Benedetti, Paola Gervasio, Davide Luscietti, Mariagrazia Pilotelli & Adriano Maria Lezzi

To cite this article: Marta Benedetti, Paola Gervasio, Davide Luscietti, Mariagrazia Pilotelli & Adriano Maria Lezzi (2018): Point Thermal Transmittance of Rib Intersections in Concrete Sandwich Wall Panels, Heat Transfer Engineering, DOI: 10.1080/01457632.2018.1457208

To link to this article: https://doi.org/10.1080/01457632.2018.1457208

Accepted author version posted online: 26 Mar 2018.
Published online: 12 Apr 2018.

HEAT TRANSFER ENGINEERING
2018, VOL. 0, NO. 0, 1–10
https://doi.org/10.1080/01457632.2018.1457208

Taylor & Francis
Taylor & Francis Group

Point Thermal Transmittance of Rib Intersections in Concrete Sandwich Wall Panels

Marta Benedetti[a], Paola Gervasio[b], Davide Luscietti[c], Mariagrazia Pilotelli[c], and Adriano Maria Lezzi[c]

[a]Dipartimento di Ingegneria dell'Informazione, Università degli Studi di Brescia, Brescia, Italy; [b]Dipartimento di Ingegneria Civile, Architettura, Territorio, Ambiente e di Matematica, Università degli Studi di Brescia, Brescia, Italy; [c]Dipartimento di Ingegneria Meccanica e Industriale, Università degli Studi di Brescia, Brescia, Italy

ABSTRACT

Concrete sandwich panels are building elements made by two concrete wythes separated by a layer of lightweight material: the central layer is inhomogeneous due to the presence of concrete ribs which tie the external wythes and act as thermal bridges. This paper deals with the problem of determining point thermal transmittance associated with rib intersections. Together with previous results by the authors, it allows accurate calculation of thermal transmittance of sandwich panels according to current International Standards. A dataset of 1080 point transmittance values is obtained upon use of a spectral element method, varying systematically material conductivities and thickness of panel layers, for the most common pairs of rib widths in current panel production. To limit the computational cost, a solution strategy based on the use of low-order polynomials on three grids of increasing refinement, coupled with Richardson extrapolation is adopted. Finally, a power law correlation is proposed that allows to estimate point transmittance within a relative error of 10%.

Introduction

Precast concrete sandwich wall panels are building elements that allow fast and economical constructions of buildings such as factories, warehouses, and malls: these panels are designed to span from the foundation to the roof and can be used as load bearing walls, or exterior claddings, or both. Since panels are usually produced far from the construction site, weight becomes a crucial point with regard to handling, transportation, and installation issues. The easiest way to meet both the requirements of structure robustness and weight containment, is to have a frame of concrete and fill the empty zones with lightweight materials like expanded polystyrene. In what follows, this kind of panel will be referred to as precast concrete lightened sandwich wall panel (LSP). It is worth underlining that the use of insulating slabs in LSP, which is aimed to reduce weight, does reduce the average thermal transmittance of the panel at the same time. There are other types of sandwich panels much more thermal efficient than LSP because of the presence of a continuous layer of homogeneous insulations between the concrete wythes (insulated sandwich wall panel): they are not considered here since the computation of their thermal transmittance is straightforward.

In a LSP, two prestressed concrete wythes are separated by a heterogeneous layer made by lightweight slabs and concrete ribs: so there are panel regions made of solid concrete which act as thermal bridges. Building designers in order to fulfill the requirements of the European directives on the energy performance of buildings (Directives 2002/91/EC and 2010/31/EU) as implemented by the EU member states, need reliable estimates of the thermal transmittance of building elements, including the effects of thermal bridges. In principle, computation of the thermal transmittance U of LSPs is not a critical issue: ISO 6946, ISO 14683, and ISO 10211 [1]–[3] describe accurate methods to do that. These methods require the knowledge of linear and point thermal transmittances associated with thermal bridges in LSPs. Their values can be computed upon numerical simulations performed as described in ISO 10211 [3]. However, most panel manufacturers are small-medium enterprises (SMEs) and their technical staff does not have either the know-how or the time to numerically compute values necessary to determine the transmittance U of their product range: they consider much more convenient the usage of transmittance catalogs or correlations easily implemented in a spreadsheet or in an in-house code.

Other recent studies [4], [5] pursue a goal similar to this study, that is to find correlations to evaluate thermal properties of building components which satisfy the following requirements: they must reproduce with good

CONTACT Professor Adriano Maria Lezzi adriano.lezzi@unibs.it Dipartimento di Ingegneria Meccanica e Industriale, Università degli Studi di Brescia, via Branze 38, 25123 Brescia, Italy.

approximation the results of standardized methods; in addition, they must be suited for routine use in industry. Tenpierik et al. [4] propose a closed analytical model for calculating linear transmittances in vacuum insulation panels that is much more accurate than models based on electric circuits, but less laborious than numerical simulations. Buratti et al. [5] develop an artificial neural network (ANN) for estimating U of wooden framed windows. Based on 278 experimental and numerical data obtained in accordance with standards, the ANN returns an estimate of window transmittance as a function of 10 simple parameters like window typology, wood kind, frame thickness, etc.

In a companion paper [6], the problem of finding an accurate correlation for prediction of linear thermal transmittance values of LSPs was addressed. The goal was reached through the combined use of a fast and accurate spectral element method (SEM) and of an ANN. The SEM allowed the authors to obtain a large dataset of linear transmittance values and then they used it to train the ANN. In this work, the study investigating the point thermal bridges in LSPs and determining the associated point thermal transmittance was completed.

Point thermal bridges in LSPs coincide with concrete rib intersections, like in the four panel corners. ISO 14683 [2, Clause 5.3.2] states that, in general, the effect of point thermal bridges "insofar they result from the intersection of linear thermal bridges," can be neglected. In past years, in a few real cases point thermal bridge contribution in LSPs was evaluated by the authors and it was found that it accounted for up to 2%, approximately. Besides, the associated point transmittances were negative: neglecting them implied overestimating panel transmittance U. In this work, the correctness and the generality of these conclusions were checked, on the basis of a systematic study of point transmittance as a function of concrete and lightweight material conductivities and panel geometrical parameters.

Evaluation of point thermal transmittance requires three dimensional (3D) numerical simulations, besides the knowledge of linear transmittance associated with the intersecting concrete ribs. As in [6], a conformal quadrilateral SEM is used: the computational effort required to approximate point transmittances is much larger than that needed to estimate linear ones. That forces the use of coarse meshes and to approximate the temperature field in each mesh element with low-order polynomials, but with the major drawback of loss of accuracy. Here, a solution strategy that allows to by-pass this problem is presented and discussed. The numerical problem is solved on three grids of increasing refinement – although overall rather coarse – upon use of low-order polynomials ($p = 4$): results are extrapolated by Richardson method [7], [8]. This procedure assures a good trade-off between accuracy, as required by International Standards, and computational cost.

A dataset of point transmittance values is obtained varying systematically material conductivities and thickness of external and central layers, for the most frequent pairs of rib widths in current panel production. A simple power law correlation in terms of a new variable depending on linear transmittances and concrete wythes thickness has been proposed in this study. This correlation allows to estimate point transmittances within a relative error of $\pm 10\%$ which is intermediate between the typical accuracy of numerical calculation of linear thermal transmittance ($\pm 5\%$) and that of linear thermal bridge catalogs ($\pm 20\%$), as stated in ISO 14683 [2, Clause 6.4].

In the literature there are only a few other studies on point thermal bridges in precast concrete panels: all of them consider insulated sandwich wall panels and not LSPs. An insulated sandwich wall panel is characterized by a continuous layer of insulation between the outer concrete wythe and the inner one. The two wythes are tied together by connectors (usually metal ones). Since the connectors pass through the insulation layer, they act as point thermal bridges. Studies [9]–[11] are concerned with the thermal effect of metal connectors used in insulated sandwich wall panels.

Lee and Pessiki [9] propose a modified algebraic method to estimate point transmittance associated to wythe connectors made of steel wires. Their results are verified by comparison with 3D finite element solutions.

Willems and Hellinger [10] propose a correlation for point transmittance of metal connectors. Their results are based on numerical computations and apply to four types of connectors produced by German manufacturers.

Kim and Allard [11] present an experimental and finite element study of three types of steel wire connectors, considering the effect of shape and spacing.

To the authors' knowledge, therefore, this paper is the only one that tries and proposes a practical correlation for calculation of point transmittance associated with rib intersections in LSP.

Average thermal transmittance of a lightened sandwich panel

The heat flow rate q through a wall panel can be usually written as

$$q = AU\Delta T \tag{1}$$

where ΔT is the temperature difference between the internal and the external environments separated by the panel, A is the panel area, and U is the panel average thermal transmittance. In Eq. (1), which defines U, the four panel edges are considered adiabatic.

Although q could be calculated upon numerical solution of the conduction equation for the entire panel, International Standards [2], [3] suggest a more efficient method based on analytical and numerical solutions for a limited number of parts of the panel. Following this approach, q is written as

$$\frac{q}{\Delta T} = AU = \sum_i A_i U_i + \sum_j l_j \psi_j + \sum_k n_k \chi_k \qquad (2)$$

In Eq. (2) A_i and U_i are area and thermal transmittance of the i-th *section* of the panel; l_j and ψ_j are length and linear transmittance of the j-th linear thermal bridge; n_k and χ_k are number and point transmittance of the k-th point thermal bridge. Following ISO 6946 [1, Clause 6.7.2.2], here *section* denotes a panel part made of thermally homogeneous layers. As clearly shown in Figure 1, a LSP is made of two *sections*: the solid concrete part, corresponding to ribs (*section a*); and the three-layer lightened part, made of the concrete wythes and the lightened layer that separates them (*section b*).

The thermal transmittance of the two *sections*, U_a and U_b, is easily calculated in terms of surface resistances, R_{se} and R_{si}, and of thermal resistances of the homogeneous layers. Therefore, the first sum in Eq. (2), $\sum_i A_i U_i$ represents the transmission heat coefficient through the panel as if the *sections* were thermally insulated one from the other, and the temperature field was 1D within each *section*.

The other two sums, $\sum_j l_j \psi_j$ and $\sum_k n_k \chi_k$, represent the corrections associated with linear and point thermal bridges, that is with the regions where the temperature field is two dimensional (2D) and 3D.

In LSPs, the temperature field is closely approximated by a 2D field near the interfaces between concrete ribs and lightweight slabs (thick lines in Figure 1), whereas it is fully 3D in a neighborhood of the intersections of ribs (open circles in Figure 1).

The linear thermal transmittances ψ_j must be evaluated upon solving the conduction equation on 2D domains as described in [6]. Evaluation of the point thermal transmittances χ_k – which is the goal of this study – requires solution of the conduction equation on proper 3D domains which represent panel parts centered around rib intersections. These 3D geometrical models must be identified in accordance with ISO 10211 [3].

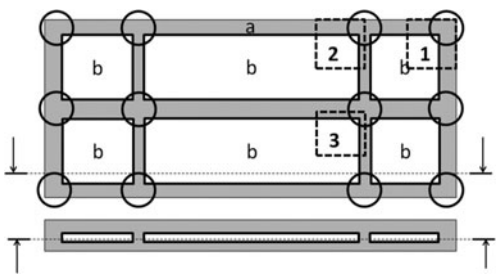

Figure 1. Plan and section view of a LSP: (a) solid concrete *section*; (b) lightened *section*. Thick lines and open circles indicate linear and point thermal bridges, respectively. Domains 1, 2, and 3 are examples of 3D models used in numerical simulations.

Point transmittance calculation

Problem Description

In Figure 2, the 3D model used to determine point thermal transmittance values is sketched: it represents the part of a panel near the intersection of two ribs. The L-shaped region formed by the intersecting ribs, represents the solid concrete *section a*, whereas the three-layered region is the lightened *section b*.

The 3D geometrical model coincides with the parallelepiped Ω of sides $L_x = L_{ax} + L_{bx}$ and $L_z = L_{az} + L_{bz}$ and height (panel thickness) $d = d_1 + d_2 + d_3$. d_1 and d_3 denote the thickness of the external and internal wythe, respectively, whereas d_2 is the lightweight material thickness.

On the domain boundaries, the following conditions must be satisfied. On the external and internal surfaces $\partial\Omega_e(y = 0)$ and $\partial\Omega_i(y = d)$ Robin condition is imposed. The heat transfer from surface $\partial\Omega_e$ to the external environment at temperature T_e is characterized by a heat transfer coefficient α_e and a surface resistance $R_{se} = 1/\alpha_e$. Internal environment temperature T_i, heat transfer coefficient α_i, and surface resistance $R_{si} = 1/\alpha_i$ characterize heat transfer to the internal surface $\partial\Omega_i$.

Planes $x = 0$, $x = L_x$, $z = 0$, and $z = L_z$ are cut-off planes as defined in ISO 10211 [3, Clause 7.2], which coincide with adiabatic surfaces: the union of all adiabatic lateral surfaces will be denoted $\partial\Omega_a$.

Boundaries $x = L_x$ and $z = L_z$ belong to either an adiabatic lateral surface of the panel (as in domains 1 and 2 in Figure 1) or a symmetry plane of an internal rib (as in domains 2 and 3 in Figure 1): therefore L_{ax} and L_{az} are either the width of a bounding rib or the half-width of an internal rib.

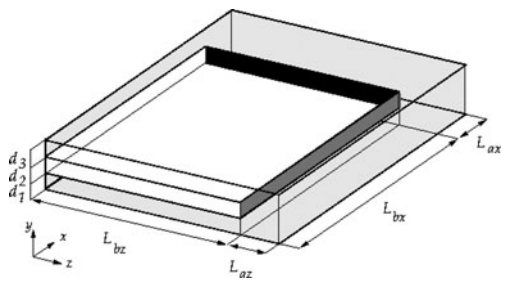

Figure 2. The computational domain Ω, the intersecting ribs form two linear and one point thermal bridges. The linear thermal transmittances are considered as associated with the black (ψ_x) and gray (ψ_z) interfaces.

Boundaries $x = 0$ and $z = 0$ are placed so far from the intersection that the temperature field on them is 2D for all practical purposes. According to ISO 10211, the distances L_{bx} and L_{bz} between the cut-off planes and the point thermal bridge must be larger or equal to max (1 m, 3 d), where d is the total thickness of the panel. Symmetry planes of lightweight slab could also be taken as cut-off plane $x = 0$ ($z = 0$, respectively) if L_{bx} (L_{bz}, respectively) is smaller than max (1 m, 3 d).

Denoting q the heat flux through the 3D domain Ω, Eq. (2) simplifies as follows:

$$\frac{q}{\Delta T} = A_a U_a + A_b U_b + L_{bz}\psi_x + L_{bx}\psi_z + \chi \qquad (3)$$

where $A_a + A_b$ is equal to the area of surfaces $\partial\Omega_e$ and $\partial\Omega_i$. ψ_x and ψ_z are the linear transmittances associated with the interfaces between concrete and lightweight material that are highlighted in black and gray, respectively, in Figure 2.

Upon numerical evaluation of q and ψ_x and ψ_z (see [6]) the point transmittance χ associated with the rib intersection modeled in Figure 2, can be computed as

$$\chi = \frac{q}{\Delta T} - (A_a U_a + A_b U_b + L_{bz}\psi_x + L_{bx}\psi_z) \qquad (4)$$

Input data

The point transmittance χ as defined by Eq. (4) depends on several parameters: geometrical, L_{ax}, L_{az}, L_{bx}, L_{bz}, d_1, d_2, d_3; and thermophysical, λ_{co}, λ_{lw}, R_{se}, R_{si}.

In this study, R_{se}, R_{si}, L_{bx}, and L_{bz} are fixed, and χ is computed for varying values of the other variables. The surface resistances are set equal to the conventional values prescribed by ISO 6946 [1, Clause 6.8]: $R_{se} = 0.04$ m^{2}K/W and $R_{si} = 0.13$ m^{2}K/W.

As observed in [6], linear transmittance ψ associated with a concrete rib tends asymptotically to a constant value as the lightweight slab length increases (L_{bx} and L_{bz} in Figure 2). As a matter of fact the growth is rapid: for length larger than 0.25 m the value of ψ is hardly distinguishable from the asymptotic value. Since in real panels the lightweight slab length and width are rarely smaller than 0.5 m, the asymptotic value only is needed for all practical purposes. A similar behavior is expected to characterize the dependence of χ on L_{bx} and L_{bz}: therefore, following ISO 10211 [3], in all computations we set $L_{bx} = L_{bz} = 1$ m.

In [6], linear transmittance ψ is computed for several thousands of different combinations of (L_a, d_1, d_2, d_3, λ_{co}, λ_{lw}). Due to the larger computational cost of 3D simulations, χ has been calculated for a subset of the dataset. Values investigated here are summarized in Table 1. In particular, only three values for both concrete and lightweight material conductivity have been considered: $\lambda_{co} = 1.6$, 2.0, and 2.4 W/mK; $\lambda_{lw} = 0.02$, 0.04, and 0.06 W/mK.

Table 1. Input data set used in computations.

Variable	Value set	Unit
λ_{co}	1.60, 2.00, 2.40	W/mK
λ_{lw}	0.02, 0.04, 0.06	W/mK
L_{ax}*	0.05, 0.10, 0.20, 1.00	m
L_{az}*	0.05, 0.10, 0.20, 1.00	m
$d_1 = d_3$**	0.04, 0.06, 0.08	m
d_2**	0.04, 0.06, 0.08, 0.12, 0.16	m

*Not all combinations are allowed: $L_{az} \leq L_{ax}$
**Not all combinations are allowed: $d = d_1 + d_2 + d_3 \leq 0.24$ m

The dependence of point transmittance on solid concrete *section* widths L_{ax} and L_{az}, is similar to the one on L_{bx} and L_{bz}: it attains its asymptotic value for L_{ax} and L_{az}, larger than 0.2 m, approximately. The three most frequent values of rib width or half-width: 0.05, 0.10, and 0.20 m have been studied. In addition, we compute also the asymptotic cases which can be approximated setting widths equal to 1 m.

With respect to Figure 2, for symmetry reasons the value of χ is invariant when L_{ax} and L_{az} commute, thus only combinations $L_{ax} \leq L_{az}$ need to be considered.

In current production of LSPs, the concrete wythes have usually the same thickness, therefore analysis has been restricted to the symmetric case $d_1 = d_3$. Three values of wythe thickness have been considered: 0.04, 0.06, and 0.08 m. They are the most frequent for panels of total thickness less than or equal to 0.24 m. Thickness of the lightened layer, d_2, has been varied among: 0.04, 0.06, 0.08, 0.12, and 0.16 m. However, the following constraint on panel total thickness has been imposed: $d \leq 0.24$ m: only 12 combinations of values of d_1 and d_2 satisfy this condition.

One thousand and eighty numerical estimates of χ have been obtained upon varying ($L_{ax}, L_{az}, d_1, d_2, \lambda_{co}, \lambda_{lw}$) as specified above.

Numerical solution

The conduction problem described in the previous section is solved through SEM. SEMs are high accurate methods designed to discretize partial differential equations. Their best performance (in terms of computational efficiency) is achieved when the differential problem is set on Cartesian geometries, exactly as in the problem we are dealing with, since SEMs exploit the tensorial structure of the basic functions. The accuracy of SEM is restricted by the regularity of the data: the thermal conductivity and the prescribed boundary conditions.

Examples of application of SEM in heat and fluid flows can be found in [12], [13]. A brief description of SEM as applied to transmittance computation in LSPs can be

found in [6, Sec. 4], whereas for an in-depth description of SEM and of its use to approximate partial differential equations, we refer, e.g., to [14], [15]. Only features and terms necessary to understand the solution strategy adopted have been presented in the study.

With respect to Figure 2, in order to approximate the heat flux q through Ω we compute the temperature $T = T(x)$ inside the panel. It solves a homogeneous elliptic equation with discontinuous thermal conductivity λ such that $\lambda|_{\Omega_{co}} = \lambda_{co}$, and $\lambda|_{\Omega_{lw}} = \lambda_{lw}$, where the nonoverlapping regions Ω_{co} and Ω_{lw} correspond to the concrete and the lightweight material, respectively.

T is the solution of

$$\begin{cases} -\nabla \cdot (\lambda \nabla T) = 0 \text{ in } \Omega, \\ \lambda \frac{\partial T}{\partial n} + \alpha_e T = \alpha_e T_e \text{ on } \partial\Omega_e, \quad \lambda \frac{\partial T}{\partial n} + \alpha_i T = \alpha_i T_i \text{ on } \partial\Omega_i, \\ \lambda \frac{\partial T}{\partial n} = 0 \text{ on } \partial\Omega_a \end{cases} \tag{5}$$

In SEM, problem (Eq. 5) is reformulated in a weak sense, and it can be proved that it admits a unique weak solution $T \in H^1(\Omega)$, being $H^1(\Omega) = \{v \in L^2(\Omega) : \nabla v \in [L^2(\Omega)]^2\}$ the Sobolev space of order 1 (see, e.g., [16]). The low regularity of the solution is a consequence of the discontinuous thermal conductivity. Nevertheless, when restricted to the subregions where the thermal conductivity is constant, the temperature field is more regular, precisely it belongs to the Sobolev space of order 2.

To approximate the temperature field inside the panel the computational domain Ω is partitioned in N nonoverlapping parallelepiped Q_k (also named elements) of size h (typically h denotes the diagonal), such that two adjacent elements share a vertex, an edge, or a complete face. Such a partition will be denoted by $Q_h = \bigcup_{k=1}^{N} Q_k$. We accept that the elements Q_k can have different size h_k, in such a case we set $h = \max_k h_k$.

Given a partition Q_h of Ω we look for an approximation T_h of T that is globally continuous on $\bar{\Omega}$ and locally (that is in each element Q_k) is a polynomial of degree p with respect to each variable. If the surfaces of discontinuity of the thermal conductivity do not cut any element Q_k, it can be proved that the discrete solution T_h converges to the weak solution T of Eq. (5) when the mesh size h tends to zero and/or the polynomial degree p grows to infinity. More precisely, there exists positive constants c_k independent of both h_k and p such that

$$\|T_h - T\|_{H^1(\Omega)} \leq \left(\sum_{k=1}^{N} c_k {h_k}^2 p^{-2} \|T\|^2_{H^2(Q_k)} \right)^{1/2} \tag{6}$$

where $H^2(Q_k)$ is the Sobolev space of order 2 [14].

Once the discrete temperature T_h is available, the heat flux through surfaces $\partial\Omega_i$ and $\partial\Omega_e$ can be computed by the following formulas:

$$\begin{aligned} q_{i,h} &= \int_{\partial\Omega_i} \lambda_{co} \frac{\partial T_h(x)}{\partial n} d\partial\Omega = \int_{\partial\Omega_i} \alpha_i (T_i - T_h)\, d\partial\Omega \\ q_{e,h} &= -\int_{\partial\Omega_e} \lambda_{co} \frac{\partial T_h(x)}{\partial n} d\partial\Omega = \int_{\partial\Omega_e} \alpha_e (T_h - T_e)\, d\partial\Omega \end{aligned} \tag{7}$$

$q_{i,h}$ and $q_{e,h}$ are the discrete approximation of the heat flux through Ω, q, that is required to calculate the point transmittance χ by Eq. (4). In particular, since both $|q_{i,h} - q|$ and $|q_{e,h} - q|$ behave like $\|T_h - T\|_{H^1(\Omega)}$ when $h \to 0$ and/or $p \to \infty$, we obtain $q_{i,h} \to q$, and $q_{e,h} \to q$ when $h \to 0$ and/or $p \to \infty$. The SEM has been implemented in MATLAB.

Discretization strategies

In order to get a good trade-off between accuracy and computational time, one has to choose properly the partition Q_h and the polynomial degree p. Since p is the same in every Q_k, in view of Eq. (6) the element size h_k should suitably be chosen in order to balance $\|T\|_{H^2(Q_k)}$, the latter being larger next to the surfaces where the thermal conductivity is discontinuous and smaller far from it.

For each set of data, and any fixed p, the discrete fluxes (Eq. 7) have been computed for three different meshes:

Q_h (named *coarse*), $Q_{h/2}$ (*medium*), and $Q_{h/4}$ (*fine*). Therefore, the corresponding point transmittances $\chi_{h,p}$, $\chi_{h/2,p}$, and $\chi_{h/4,p}$ have been evaluated by using Eq. (4) in which q is replaced by its discrete counterpart $q_h = (|q_{i,h}| + |q_{e,h}|)/2$.

Finally, $\chi_{h,p}$, $\chi_{h/2,p}$, and $\chi_{h/4,p}$ are used to better estimate the point transmittance χ through the Richardson extrapolation technique (see, e.g., [8, Eq. 9.6]), that in our case (with data from three different meshes and the parameter h that is halved at each step) reads

$$\chi_{e,p} = \frac{8\chi_{h/4,p} - 6\chi_{h/2,p} + \chi_{h,p}}{3} \tag{8}$$

In view of the convergence estimate of Richardson extrapolation (see, e.g., [8, Eq. 9.35]), there exists a positive constant C, independent of h, but possibly depending on p such that $|\chi_{e,p} - \chi| \leq C(p)(h/4)^3$. The Richardson extrapolation turns out to be very efficient for the purpose of this study. As a matter of fact, even if the SEM approximation error (Eq. 6) vanishes as h^1 when $h \to 0$ in view of the low regularity of the thermal conductivity, Richardson extrapolation allows to gain third order accuracy with respect to h, i.e., h^3, by using a set of three meshes of moderate sizes h, $h/2$, and $h/4$, instead of a unique mesh with a very small mesh-size, that would require very large computational effort.

Table 2. At left, columns 2–4, CPU-time in seconds needed to compute the temperature by SEM discretization. At right, columns 5–7, the Richardson extrapolation of the point transmittances (in W/K) for different values of p, the relative error with respect to the best computed value $\chi_{e,6}$, and the total CPU-times (in s).

p	Coarse	Medium	Fine	$\chi_{e,p}$	e_p	CPU-time
2	2.19×10^{-1}	3.06×10^{0}	6.70×10^{1}	-1.2792×10^{-2}	1.0401×10^{-2}	7.03×10^{1}
4	2.05×10^{0}	4.00×10^{1}	1.44×10^{3}	-1.2661×10^{-2}	3.8467×10^{-5}	1.48×10^{3}
6	1.27×10^{1}	2.27×10^{2}	9.81×10^{3}	-1.2660×10^{-2}	—	1.01×10^{4}

In our simulations we have chosen to use polynomial degree $p = 4$. This choice is motivated by several numerical tests, carried out to measure both the computational effort required to solve the linear system associated with the SEM discretization of the conduction problem (Eq. 5), and the accuracy of the computed point transmittance.

As test case to study discretization error and computational effort, we have chosen the case: $L_{ax} = L_{az} = 0.05$ m, $d_1 = d_3 = 0.06$ m, $d_2 = 0.12$ m, $\lambda_{co} = 2.0$ W/mK, $\lambda_{lw} = 0.04$ W/mK, and on the associated geometry we have designed the following partitions.

The *coarse* partition or mesh Q_h is obtained by defining $6 \times 4 \times 6$ (= 144) elements with side sizes $h_x = [0.6, 0.2, 0.1, 0.05, 0.05, | 0.05]$, $h_y = [0.06, | 0.06, 0.06, | 0.06]$, and $h_z = h_x$. The symbols | highlight where the thermal conductivity is discontinuous. The ratio between the maximum and the minimum size h_k is about 10, with $\max_k h_x \simeq 0.85$ and $\min_k h_x \simeq 0.09$. The *medium* mesh $Q_{h/2}$ is obtained by halving (along each direction) any element of Q_h, therefore we have $12 \times 8 \times 12$ (= 1,152) elements; while the *fine* mesh $Q_{h/4}$ is obtained by halving (along each direction) any element of $Q_{h/2}$, here we have $24 \times 16 \times 24$ (= 9,216) elements.

The linear system arising from the SEM discretization of Eq. (5) has dimension close to $p^3 N$ and the matrix is very sparse, therefore it is mandatory to solve it by an iterative method, like, e.g., the Bi-CGStab method [10], preconditioned by an incomplete LU factorization.

The CPU-times (in seconds) needed to compute the temperature field on an Intel i5-3470 4 core, 64 bit, 3.6 GHz, and 8 GB of RAM, are reported in Table 2, (left), for $p = 2, \ldots, 6$ and the three partitions Q_h, $Q_{h/2}$, and $Q_{h/4}$. Least square approximation of the measured values provides CPU-time $\simeq 10^{-7} p^{5.6} N^{1.7}$ s. It can be concluded that a large computational effort is required to solve Eq. (5) when either moderate or large p is used.

To measure the accuracy of numerical results, the Richardson extrapolation of the point transmittance $\chi_{e,p}$ was computed, for any $p = 2, 4, 6$, as well as the relative error with respect to $\chi_{e,6}$ (the best estimate), i.e.,

$$e_p = \frac{|\chi_{e,p} - \chi_{e,6}|}{|\chi_{e,6}|} \tag{9}$$

The computed point transmittances $\chi_{e,p}$, the errors (9), and the CPU-times needed to estimate $\chi_{e,p}$ (i.e., the total CPU-time needed to compute the discrete temperature on all three meshes) are shown in Table 2, (right). It can be concluded that the best compromise, obtained by minimizing both the CPU-time and the error is achieved for $p = 4$.

Results and discussion

One thousand and eighty numerical estimates of χ have been obtained varying six parameters:

$$\chi = \chi\,(L_{ax}, L_{az}, d_1, d_2, \lambda_{co}, \lambda_{lw}) \tag{10}$$

The interval spanned by χ over the set of input data ranges between -4.38×10^{-2} and -0.48×10^{-2} W/K: all values are negative. There is no evidence that the dependence of χ on some of the variables could be neglected because it is much weaker than others.

With respect to Figure 3, it was observed that χ is a decreasing function of d_1 (see Figure 4 also) and of λ_{co}, whereas it is an increasing function of λ_{lw}: the rate of change does depend on the other variables, but it is always significant. Dependence on d_2 may be considered less stronger, however that is only because χ distributes around a relative minimum centered at $d_2 < 0.08$ m (see, e.g., Figure 4). In other regions of the input data space investigated here, there is no evidence of the minimum and χ is an increasing function of d_2 (see, e.g., Figure 5).

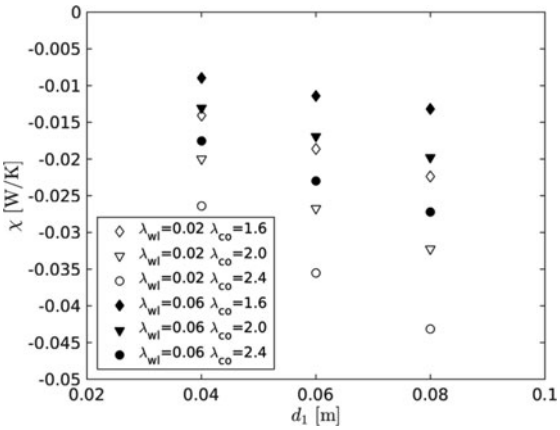

Figure 3. χ vs. d_1 for $\lambda_{co} = 1.6$ (♦,◊), $\lambda_{co} = 2.0$ (▼,∇), $\lambda_{co} = 2.4$ (●,○), and $\lambda_{lw} = 0.02$ (open marks), $\lambda_{lw} = 0.06$ (solid marks). λ's in [W/mK]. $L_{ax} = L_{az} = 0.2$ m, $d_2 = 0.04$ m. The strong dependence of χ on the selected parameters is apparent.

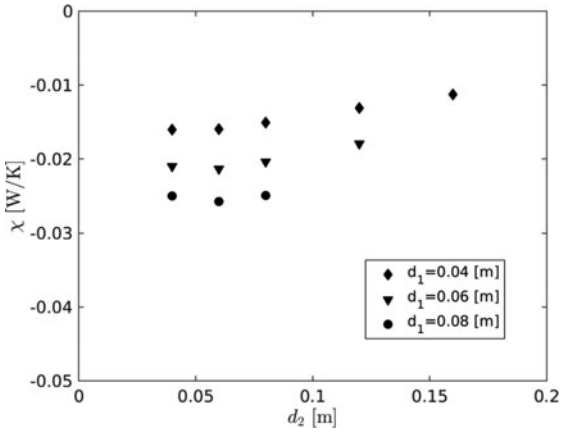

Figure 4. χ vs. d_2 for different d_1. $L_{ax} = L_{az} = 0.2$ m, $\lambda_{co} = 2.0$ W/mK, $\lambda_{lw} = 0.04$ W/mK. For this choice of inputs χ shows a minimum.

Finally, with respect to Figure 5 it was observed that χ tends quite fast to an asymptotic value for L_{ax} and L_{az} tending to infinity, so that values for $L_{ax} = L_{az} = 0.2$ m almost coincide with those for $L_{ax} = L_{az} = 1$ m. However, when one or both rib widths are equal either to 0.05 or 0.1 m, χ attains a larger value.

In recent years, ANN have been used in heat transfer studies to obtain accurate correlations for either heat transfer coefficient or other thermal quantities, as in [17], [18]. Indeed, at the beginning of this study it was planned to develop an ANN for prediction of χ, as was done for ψ in [6]. However, in [6] to train an ANN able to model correctly the dependence on L_a, values of ψ for more than 10 L_a between 0.05 and 1 m had to be obtained. In this study, computational cost of tens of (L_{ax}, L_{az}) pairs was not affordable. Nor it seemed useful to develop an ANN for each pair (L_{ax}, L_{az}) investigated. A different approach was followed.

According to ISO 14683 [2], the point thermal bridge studied here can be considered as the intersection

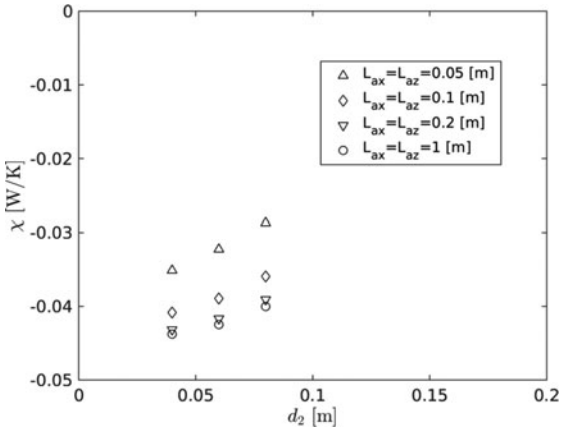

Figure 5. χ vs. d_2 for different (L_{ax}, L_{az}) pairs. $d_1 = 0.08$ m; $\lambda_{co} = 2.4$ W/mK; and $\lambda_{lw} = 0.02$ W/mK. χ tends quite fast to an asymptotic value as rib width increases: values for $L_{ax} = L_{az} = 0.2$ m coincide with those for $L_{ax} = L_{az} = 1$ m.

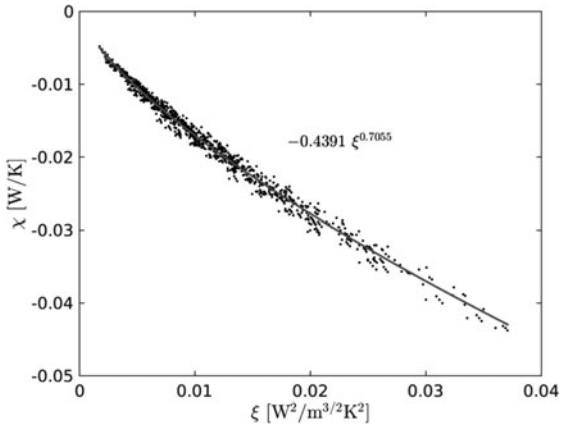

Figure 6. All computed values of χ vs. the variable $\xi = \psi_x \psi_z \sqrt{2d_1}$. Solid line: least square approximation of data through a power law.

of two linear bridges associated with transmittances $\psi_x(L_{ax}, d_1, d_2, \lambda_{co}, \lambda_{lw})$ and $\psi_z(L_{az}, d_1, d_2, \lambda_{co}, \lambda_{lw})$: variable d_3 is not listed since only the case $d_3 = d_1$ is being considered. It was thought whether the dependence of χ on the six variables could be captured to some extent by ψ_x and ψ_z, that is whether χ depend implicitly on $(L_{ax}, L_{az}, d_1, d_2, \lambda_{co}, \lambda_{lw})$ through ψ_x and ψ_z:

$$\chi = g(\psi_x, \psi_z) \tag{11}$$

For symmetry reason in Eq. (11) ψ_x and ψ_z must commute, that is g has to depend on commutative functions of ψ_x and ψ_z, such as $\psi_x \psi_z$, $\psi_x + \psi_z$, etc.

As a matter of fact, if computed values of χ are plotted versus $\psi_x \psi_z$ data tend to fall within a smooth narrow region of increasing width for increasing $\psi_x \psi_z$. Data dispersion depends on the original variables, but dependence on d_1 seems stronger. After a few trials, the following new variable was obtained:

$$\xi = \psi_x \psi_z \sqrt{2d_1} \tag{12}$$

for which dispersion is substantially reduced (see Figure 6). Although factor 2 multiplying d_1 is clearly unnecessary, it was preferred to introduce it because it was believed that for the more general case $d_3 \neq d_1$, variable ξ should be defined as $\xi = \psi_x \psi_z \sqrt{(d_1 + d_3)}$. Upon fitting data with a power law, the following correlation for point transmittance has been obtained:

$$\chi_c(\xi) = -0.4391 \xi^{0.7055} \tag{13}$$

where all quantities are in SI units.

For all practical purposes Eq. (13) supplies a rather good estimate of χ when the linear transmittances associated with the intersecting ribs are known. In Figure 7 the point transmittance estimated by correlation (Eq. 13), χ_c, is plotted versus the computed value χ: 97% of estimates fall within $\pm 10\%$ band.

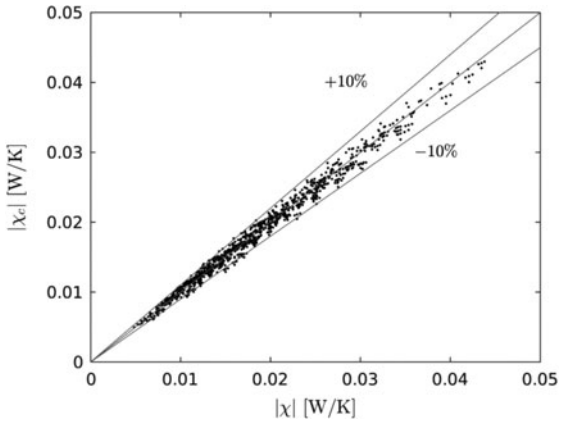

Figure 7. Comparison between correlation predictions, $|\chi_c|$, and computed data $|\chi|$: 97% of estimates fall within ±10% band.

Eq. (13) on average neither overpredicts nor underpredicts significantlyχ, since the mean relative deviation, MRD, is equal to 0.09%. Dispersion of predicted values is limited since the standard deviation, SD, is equal to 4.5%. Here, SD is defined in terms of relative deviation $\mathrm{RD} = (\chi_c - \chi)/\chi$:

$$\mathrm{SD} = \sqrt{\frac{1}{N-1}\sum\nolimits_i (\mathrm{RD}_i - \mathrm{MRD})^2} \qquad (14)$$

As mentioned in the Introduction, the relative contribution of point thermal bridges to the average panel transmittance U (term $\sum_k n_k \chi_k$ in Eq. 2) is up to 2%, approximately. Therefore, the error introduced upon use of correlation (Eq. 13) is up to 0.2% of U. This error is of the same order of magnitude as the one introduced upon use of the ANN of [6] for determining linear bridges contribution (term $\sum_j l_j \psi_j$).

Due to the small contribution of point thermal bridges in Eq. (2), one may wonder whether it would be worth to perform some 3D numerical simulations to determine them: indeed, ISO 14683 [2] does allow to neglect them. However, if one has already determined the linear transmittances of the panel ψ_j to evaluate the second term in Eq. (2), it is straightforward use of correlation (Eq. 13) to determine all point thermal transmittances and to calculate a better estimate of U. Besides, since the point thermal transmittances are always negative, taking them into account prevents panel manufacturers from overestimating the transmittance of their products.

Conclusions

This paper deals with the problem of determining point thermal transmittance associated with rib intersections in LSPs. Together with results presented in [6] it allows accurate calculation − within ±1% − of nominal average thermal transmittance of LSPs according to current International Standards [1]–[3].

To reach this goal, a dataset of point thermal transmittance associated with rib intersections of LSPs has been built through numerical simulations. One thousand and eighty data have been obtained as a function of six parameters: rib widths, thickness of the concrete wythes and of the internal layer, concrete and lightweight material conductivity. The parameters span a range of values typical of current LSPs production. To the authors' knowledge these are the only systematic data of point transmittances in concrete wall panels in literature. In general, ISO 14683 allows to omit point thermal bridge contribution to LSPs transmittance. For the input data investigated here it is shown that this contribution is always negative: one stays on the safe side neglecting it when evaluating thermal performance of LSPs. Besides, point transmittance values are rather small, their order of magnitude being 10^{-2} W/K.

Accurate calculation of such a small quantity through numerical solution of heat conduction equation in a 3D domain has been tricky and required a solution strategy based on Richardson extrapolation. A conformal quadrilateral SEM implemented in MATLAB has been used to solve the 3D conduction problem. To contain the computational effort required to solve such a problem, the unknown temperature field has been approximated using low-order polynomials, $p = 4$, with a consequent significant loss of accuracy. To bypass this problem and improve accuracy, each problem has been solved on three partitions of different degrees of refinement, starting from a very coarse partition: results have been improved through an iterated application of Richardson extrapolation. This procedure allowed to determine point transmittance values with a relative error which is about 10^{-4}.

Finally, an explicit correlation is proposed for prediction of point transmittance. Although data show a significant dependence of χ on each of the six variables mentioned above, a simple power law correlation was found which allowed to calculate χ as a function of a single variable, $\xi = \psi_x \psi_z \sqrt{2 d_1}$. The correlation has standard deviation equal to 4.5% and predicts more than 97% of computed data within ±10%. It represents a good practical tool, easily implemented in a spreadsheet or in an in-house code for calculation of U.

Nomenclature

A	panel area or *section* area, m^2
ANN	artificial neural network
a	*section* corresponding to the solid concrete part of the panel
b	*section* corresponding to the lightened part of the panel
C	constant
d	panel thickness or layer thickness, m

e_p	relative error according to Eq. (9)
H^1, H^2	Sobolev space of order 1 or 2
h	size of mesh elements, m
l	length of a linear thermal bridge, m
L	length of *sections*, m
L^2	space of square-integrable functions
L_{ax}	length of *section a* along direction x, m
L_{bx}	length of *section b* along direction x, m
L_{az}	length of *section a* along direction z, m
L_{bz}	length of *section b* along direction z, m
LSP	precast concrete lightened sandwich wall panel
MRD	mean relative deviation
n	number of the point thermal bridges
N	number of mesh (partition) elements
p	polynomial degree with respect to each variable
q	heat flow rate, W
Q_k	mesh (partition) for the computational domain
Q	mesh element
R	thermal resistance, m^2K/W
RD	relative deviation
SD	standard deviation
SEM	spectral element method
T	temperature, K
ΔT	temperature difference, K
U	thermal transmittance, W/m^2K
x	Cartesian axis direction, m
y	Cartesian axis direction, m
z	Cartesian axis direction, m

Greek Symbols

α	heat transfer coefficient, W/m^2K
λ	thermal conductivity, W/mK
ξ	auxiliary variable
χ	point thermal transmittance, W/K
χ_c	approximate point thermal transmittance computed by correlation (Eq. 13), W/K
$\chi_{e,p}$	point thermal transmittance computed by Richardson extrapolation (Eq. 8), W/K
ψ	linear thermal transmittance, W/mK
ψ_x	linear thermal transmittance associated with interface orthogonal to x, W/mK
ψ_z	linear thermal transmittance associated with interface orthogonal to z, W/mK
Ω	computational domain
$\partial\Omega$	boundary of the computational domain

Subscripts

a	referring to the solid concrete *section*
b	referring to the lightened *section*
co	concrete
e	external
h	referring to mesh size
i	internal
lw	lightweight material
p	referring to polynomial degree
se	external surface
si	internal surface

Notes on contributors

Marta Benedetti received her Master in Electrical Engineering from University of Brescia, 2015, in investigating and implementing a Spectral Element Method to determine point transmittances in concrete sandwich panels. While attending her Master program she spent 6 months at the UPV Universitat Politècnica de València, Spain, taking courses in Electronics and Telecommunications. In 2015 she joined Accenture Italia as a Security Analyst. Currently, she is involved in the design and implementation of a new security infrastructure for the Internet Banking services of one of the biggest Italian banks.

Paola Gervasio graduated in Mathematics at the "Università Cattolica del Sacro Cuore" (Italy) in 1990. She received her Ph.D. in Mathematics from the University of Milano (Italy), in 1995. She spent one year (1992–1993) as Ph.D. student at the CRS4 (Center for Advanced Studies, Research and Development in Sardinia) in Cagliari (Italy). She became researcher (1996) and then Associate Professor in Numerical Analysis (2005) at the University of Brescia (Italy). Her research interests include: numerical approximation of PDE's by either Spectral Methods, FEM and hp-FEM; Domain Decomposition Methods; Optimal Preconditioners for Spectral Methods; Stabilized numerical methods for Navier–Stokes equations; Algebraic Fractional Step methods for Navier–Stokes equations; Heterogeneous couplings of PDE's (e.g., Stokes–Darcy equations for the simulation of filtration of fluids in porous media); Domain Decomposition Methods for nonconforming discretizations, Optimal Control for PDE's. She is co-author of two books on Scientific Computing and Numerical Analysis published by Springer (one of which was translated in four languages).

Davide Luscietti graduated in Mechanical Engineering at the University of Brescia (Italy) in 2006. He worked for one year for a ship building company and, after that, he joined the Ph.D. program in Mechanical Engineering at the University of Brescia that he concluded in 2012. From 2012 to 2016 he worked as a post-doc in the Thermal Sciences group at the University of Brescia addressing problems such as: evaluation of building components thermal performances; purification of drinking water in developing countries; fire prevention in wood roof crossed by exhaust

chimney. Currently, he works in the R&D department of a wheel factory and is responsible for optimization of heat transfer during the casting process.

Mariagrazia Pilotelli graduated in Mechanical Engineering at the University of Brescia (Italy) in 1995. She received her Ph.D. in Energy from the Polytechnic University of Milano (Italy), in 2000. In 1999 she joined the Department of Mechanical Engineering of the University of Brescia (Italy) as Researcher. Her research interests span from heat transfer to applied thermodynamics, including: solidification of binary alloys; single phase convective heat transfer; heat transfer in industrial processes; heat transfer in buildings; energy access in developing countries.

Adriano M. Lezzi graduated in Physics at the University of Milan (Italy) in 1985. He received his Ph.D. in Mechanical Engineering from the Johns Hopkins University, Baltimore (USA) in 1990. He spent one year (1990–1991) as post-doc at the Institute for Numerical Analysis of National Research Council, in Pavia (Italy). In 1991 he joined the Department of Mechanical Engineering of the University of Brescia (Italy), at first as Researcher, then as Associate Professor (1997). Since 2001, he has been a Full Professor of Thermal Sciences. His research interests span from heat transfer to fluid dynamics. Some of the topics he has addressed are: critical heat flux in capillary tubes; solidification and melting with convection; free convective heat transfer; bubble dynamics; air entrainment; free surface flows; flow instabilities. Currently he is working on biomass fueled stoves, methods for evaluating building components transmittance and convective heat transfer induced by spinodal decomposition.

References

[1] ISO. "6946:2017 Building components and building elements – Thermal resistance and thermal transmittance – Calculation method".

[2] ISO. "14683:2017 Thermal bridges in building construction – Linear thermal transmittance – Simplified methods and default values".

[3] ISO. "10211:2017 Thermal bridges in building construction – Heat flows and surface temperatures – Detailed calculations".

[4] M. Tenpierik, W. Van Der Spoel, H. Cauberg, "An analytical model for calculating thermal bridge effects in high performance building enclosure," *J Build Phys.*, vol. 3, no. 4, pp. 361–387, 2008. doi: 10.1177/1744259107088008.

[5] C. Buratti, L. Barelli, E. Moretti, "Application of artificial neural network to predict thermal transmittance of wooden windows," *App Energy.*, vol. 98, pp. 425–432, 2012. doi: 10.1016/j.apenergy.2012.04.004.

[6] D. Luscietti, P. Gervasio, and A. M. Lezzi, "Computation of linear transmittance of thermal bridges in precast concrete sandwich panels," *J Phys: Conf. Ser.*, vol. 547, no. 1, Paper 012014, pp. 1–10, 2014. doi: 10.1088/1742-6596/547/1/012014.

[7] C. J. Roy, "Review of discretization error estimators in scientific computing," presented at the 48th AIAA Aerospace Sciences Meeting, Orlando, FL, AIAA Paper 2010–126, 4–7 Jan. 2010.

[8] A. Quarteroni, R. Sacco, and F. Saleri, *Numerical Mathematics*, 2nd ed. Berlin: Springer-Verlag, 2007.

[9] B.-J. Lee and S. Pessiki, "Revised zone method R-value calculation for precast concrete sandwich panels containing metal wythe connectors," *PCI J.*, vol. 53, no. 5, pp. 86–100, 2008. doi: 10.15554/pcij.09012008.86.100.

[10] W. Willems and G. Hellinger, "Exakte U-Werte von Stahlbeton-Sandwichelementen," *Bauphysik.*, vol. 32, no. 5, pp. 275–287, 2010. doi: 10.1002/bapi.201010031.

[11] Y. J. Kim and A. Allard, "Thermal response of precast concrete sandwich walls with various steel connectors for architectural buildings in cold regions," *Energy Build.*, vol. 80, pp. 137–148, 2014. doi: 10.1016/j.enbuild.2014.05.022.

[12] N. Ghaddar and A. El-Hajj, "Numerical study of heat transfer augmentation of viscous flow in corrugated channels," *Heat Transfer Eng.*, vol. 21, no. 5, pp. 35–46, 2000. doi: 10.1080/01457630050127937.

[13] M. Raisee and N. Vahedi, "Prediction of gas flow through short and long 2-d micro- and nanochannels using a generalized slip model," *Heat Transfer Eng.*, vol. 31, no. 8, pp. 675–681, 2010. doi: 10.1080/01457630903466662.

[14] C. Canuto, M. H. Hussaini, A. Quarteroni, and T. A. Zang, *Spectral Methods. Evolution to Complex Geometries and Applications to Fluid Dynamics*. Berlin: Springer-Verlag, 2007.

[15] A. Quarteroni, *Numerical Models for Differential Problems*, 2nd ed. Mailand: Springer-Verlag, 2014.

[16] A. Quarteroni and A. Valli, *Numerical Approximation of Partial Differential Equations*. Berlin: Springer-Verlag, 1994.

[17] L. M. Tam, A. J. Ghajar, and H. K. Tam, "Contribution analysis of dimensionless variables for laminar and turbulent flow convection heat transfer in a horizontal tube using artificial neural network," *Heat Transfer Eng.*, vol. 29, no. 9, pp. 793–804, 2008. doi: 10.1080/01457630802053827.

[18] T. K. Hotta and S. P. Venkateshan, "Optimal distribution of discrete heat sources under natural convection using ANN-GA based technique," *Heat Transfer Eng.*, vol. 36, no. 2, pp. 200–211, 2015. doi: 10.1080/01457632.2014.909222.